THE APPLICATION OF TiO_2 NANOPARTICLES ON WASTEWATER TREATMENT

TIAN YING

NATIONAL UNIVERSITY OF SINGAPORE

2015

THE APPLICATION OF TiO_2 NANOPARTICLES ON WASTEWATER TREATMENT

TIAN YING

(M.Sc., Peking University)

A THESIS SUBMITTED

FOR THE DEGREE OF MASTER OF SCIENCE

DEPARTMENT OF CHEMISTRY

NATIONAL UNIVERSITY OF SINGAPORE

2015

DECLARATION

I hereby declare that this thesis is my original work and it has been written by me in its entirety.

I have duly acknowledged all the sources of information which have been used in the thesis.

This thesis has also not been submitted for any degree in any university previously.

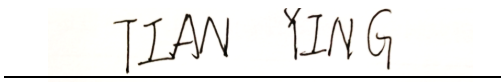

TIAN YING

10 December 2015

ACKNOWLEDGEMENTS

First of all, grateful acknowledgement is made to my dear supervisor, Prof. Chin Wee Shong, who gives me great guidance, help and suggestions during my academic year in Singapore. Because it is the first time for me to go abroad and take up a rather different major - Chemistry, I have met with a lot of challenges. Every time I feel puzzled and sad, Prof. Chin would come firstly and give me considerable help and encouragement. I am deeply touched by her patience and kindness.

Secondly, special thanks go to Prof. Gin Yew-Hoong Karina who co-supervises me and provides considerable help for my experiment. Here, I would like to express my gratitude and best wishes to Prof. Gin.

Besides, my sincere thanks should also go to my teammates in the lab, including Dr. Wang, Chen Jiaxin, Yu Miao, Doreen and Su Xinran. All of you have devoted a considerable portion of time to helping me doing experiment and solving problems. With your company, I don't feel lonely in Singapore and receive lots of love from you. Good memory will be left for me in my whole life.

Finally, I would like to thank my dear families and friends. We are living in a rather lovely family. I love all of you for giving me courage and supports all the time.

TABLE OF CONTENTS

SUMMARY

TiO_2 is a potential photocatalyst in wastewater treatment. In order to extend its application in green buildings, the combination of TiO_2 nanoparticles (P25) and PVA (poly-vinyl alcohol) was studied as hybrid films of high photocatalytic efficiency and good transparency property. It was hypothesized that organic materials and bacterial in wastewater could be removed to some extent by running the wastewater through these films.

In order to obtain better performance of these hybrid films, optimization was made from four aspects, including (i) curing temperature, (ii) film thickness (obtained through a certain amount of dropcast volume), (iii) the feed ratio of P25/PVA and (iv) the solution volume used in the synthesis process. Results indicated that the optimum film performance was obtained with 150℃, 0.25 mL drop volume, 1:1 P25/PVA and 30 mL solution volume. Under these specific conditions, 10 mg/L methylene blue (MB, 30 mL) could be decomposed to less than 15% within 120 min. Other preparation conditions yielded hybrid films that had poor stability or transparency and low photocatalytic efficiency. At higher temperature treatment, the films turned to yellow or even brown color and showed nearly no photocatalysis ability, which may suggest that the active sites of the photocatalysts have been destroyed.

In addition to MB degradation, mechanical, microbial and degradation of other typical organic dyes were also conducted to better understand the performance of

these films. Films with proper treatment showed good stability even under continually stirring environment at 300 rpm for 1 day. However, the stirring rate should not exceed 400 rpm or otherwise the films would be destroyed gradually. Microbial *E.coli* was found to be killed within 45 min under sunlight irradiation in the presence of the cast hybrid films. Another organic dye molecule, Rhodamine B (RhB) solution, could also be degraded at high efficiency. Hence, we believe that with more improvement and optimization, P25/PVA hybrid films can be made into promising materials in green buildings.

LIST OF TABLES

LIST OF FIGURES

NOMENCLATURE

PVA	Poly-vinyl alcohol
E. coli	*Escherichia coli*
MB	Methylene blue
RhB	Rhodamine B
DI water	Deionized water
LB	Luria bertani
rpm	Rounds per minute
SEM	Scanning electron microscopy
UV-Vis	Ultraviolet-visible
FT-IR	Fourier translation infrared spectroscopy
ROS	Reactive oxygen species

Chapter 1 INTRODUCTION

1.1 Wastewater pollution

With rapid urbanization and industrialization, human are facing big challenges from environmental pollution and resource shortage. As shown in the United Nations world water development report, about 200,000 tons of waste were disposed in waters every day, much more than any time in the history of civilization[1]. In China for example, according to public statistics, over 100 cities are now lacking of clean water and seriously affected by wastewater containing high levels of pollutants. From a global point of view, over one out of six people has no access to clean drinking water even at this modern age[2]. It has been highly imperative to treat wastewater pollutions effectively and economically.

1.2 Wastewater treatment

Various useful methods have been adopted in wastewater treatment, ranging from chemical processes, physical processes to biological processes, such as filtration[3], reverse osmosis[4], adsorption[5], active sludge treatment[6], membrane[7], aeration[8], anaerobic digestion[9], biological recovery[10]and so on. However, most of the traditional methods suffer from some drawbacks such as high capital, high operational cost and the possibility of second pollution especially at low concentration (0-100 mg/L).

1.3 Photocatalyst reaction - TiO_2

TiO_2 is a common catalyst in photoreactions with advantages of nontoxicity, low cost and high efficiency[11]. Lan Ma-Hock et al. studied the bioavailability of TiO_2 in wistar rats and detected no obvious organ toxicity with the concentration of 5 mg/kg TiO_2[12]. That finding suggested the safe application of TiO_2 in low doses.

As a promising photocatalyst, TiO_2 has been broadly used in many areas and fields to remove various pollutants in water and air media[13-15]. Mechanisms of TiO_2 photocatalytic reaction are shown as the followings:

$$TiO_2 + hv \rightarrow TiO_2(e^- + h^+) \quad (1)$$

$$h^+ + OH^- \rightarrow OH\cdot \quad (2)$$

$$e^- + O_2 \rightarrow \cdot O_2^- \quad (3)$$

Under the irradiation of UV light, electrons (e^-) and holes (h^+) could be photoinduced and separated in TiO_2. This further generates free radicals that participate in reactions. The oxidative TiO_2 photocatalytic reaction was mainly attributed to the highly oxidizing positive holes, especially on the surface of the photocatalyst. It was widely believed that pollutants were mainly adsorbed and degraded on the surface of TiO_2[16-18]. Therefore, more surface area is preferred in real applications.

However, due to TiO_2's wide band gap (3.2 eV) and the recombination of electrons and holes, only UV light can be absorbed and low quantum yield is

observed. In order to increase the removal and recovery efficiency of TiO_2 under solar light or visible light, much research has been conducted and enormous improvements have been made from catalyst fixation and modification. For example, by adding hydrogen peroxide or ozone, the removal rate could be enhanced a lot due to the existence of electron acceptor[19]. More details of such literature work will be given in Chapter 2.

In 1995, Negishi et al. applied TiO_2 in green buildings by coating TiO_2 films on window glasses and achieve air purification[20]. Ahmad et al., on the other hand, synthesized PVA/TiO_2 membranes with good optical property and photocatalytic activity, which brought about a promising future for the application of TiO_2 in green buildings[21]. Nevertheless, until now certain parameters have not been studied yet, such as curing temperature, film thickness and other critical parameters.

1.4 Objectives of project

The main purpose of this study is to optimize P25/PVA hybrid films' performance on pollutants removal. Detailed flow chart of the project is shown in Figure 1. Results obtained from this study could provide valuable information for the application of TiO_2 nanoparticles on wastewater treatment.

Parameters examined in this study include the followings: the film curing temperature, the thickness of the resultant hybrid films, the feed ratio of P25/PVA and

the solution volume used in the synthesis process by sequence. According to the order, the optimal values obtained in the former parameters were used in the experiment of latter parameters. On the basis of the final optimum conditions, hybrid films were then evaluated in terms of its photocatalytic performance on some organic dyes, mechanical property and microbial removal.

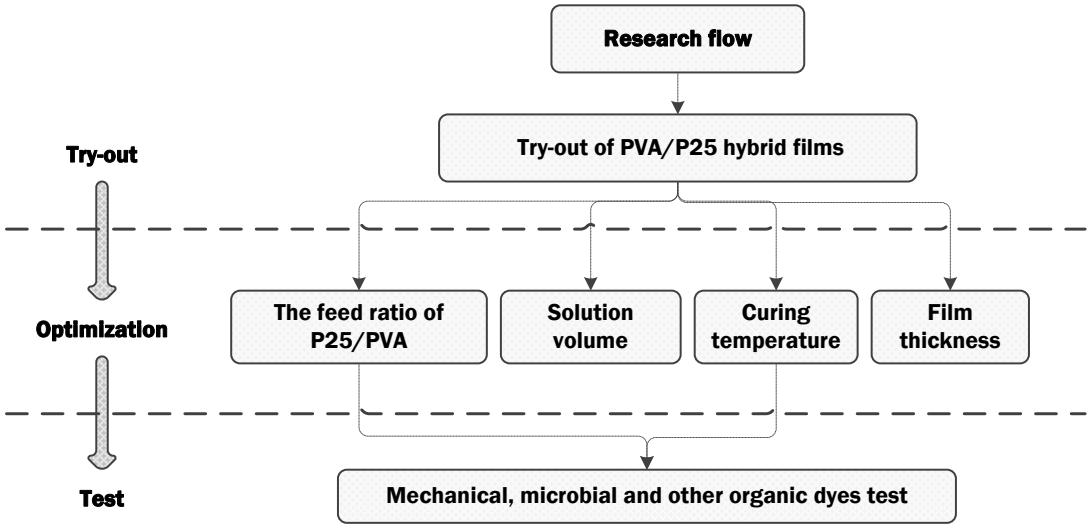

Figure 1. Flow chart of this study.

Chapter 2 LITERATURE REVIEW

2.1 Effects on TiO_2 performance

The performance of TiO_2 as photocatalyst is closely related to its crystal phase, particle size, pore structure, and other morphological properties[22]. Generally, TiO_2 prepared by various methods would contain different nanocystalline TiO_2 and they perform differently[22]. Brookite, anatase and rutile are three common phases of TiO_2, which exhibit considerably different properties in photocatalysis[23]. It was reported that TiO_2 films with mixed phases performed better than pure phase TiO_2 due to synergetic effect[24].

Besides, Anpo et al. reported that with the decrease size from 50 nm to 4 nm, higher photoactivity was observed for anatase TiO_2 nanoparticles[25]. J. F. Porter et al. investigated the effects of calcination temperature on microstructure and photoactivity of P25 (the most common type of commercially available TiO_2)[26]. Results showed that P25 treated at 923 K for 3 h had the best performance due to an increase of rutile phase and proper surface area; over thermal treatment would do detrimental harm to the photocatalytic reaction. In terms of these findings, suitable parameters for TiO_2 synthesis should be optimized.

2.2 Applications of TiO_2 in wastewater treatment

（1）TiO_2 for organic removal

Recently, the application of TiO_2 on the removal of organic, inorganic and other pollutants has attracted much research effort, as listed in Table 1. Previous research has reported that chlorinated pesticides could be degraded and mineralized through the photocatalytic reaction of TiO_2 under UV light[27, 28]. In the presence of TiO_2 at 300 nm irradiation, photocatalytic degradation of dicamba herbicide could be increased by 3 times compared with those without TiO_2 addition. The reaction rate was also somewhat related to pH change; neutral medium was more suitable than acidic or alkaline environment as the increase of hydroxide ions and charges repulsion[29].

Table 1. The application of TiO_2 on wastewater pollutants.

Radiation	Catalyst	Pollutant	Ref.
Visible light	Sandwich-structured AgCl@Ag@TiO_2	E.coli K12; Acid orange 7 dye; 2,4-dichlorophenol	[30]
UV-solar	TiO_2	EDDS, Copper	[31]
UV	TiO_2 ozonation	Benzenesulfonate	[32]
UV	Zr-N-codoped TiO_2	Phenol	[33]
UV	TiO_2/diatomite	Naproxen, Diclofenac	[34]
Solar light	TiO_2/LECA	Ammonia	[35]
UV	TiO_2	Phosphates	[36]
UV	Ag-N-TiO_2	Methanol orange	[37]

Matsushita et al. reported the successful removal of amino acid - alanine by TiO_2 addition through NMR spectroscopy[38]. Klauson et al. used TiO_2 to decompose humic acids and produced hydrogen or oxygen as a alternative energy during photocatalytic reaction process[39]. Also, TiO_2 could be applied to degrade pharmaceuticals. In Sun et al.'s experiment, naproxen and diclofenac were significantly removed in a aerated TiO_2/diatomite suspension system[40].

In spite of these applications, combining photocatalysis with other treatment methods might result in better performance due to the synergic effect. For example, Zsilák et al. removed benzenesulfonate completely by TiO_2/ozonation addition in slightly acidic environment[32].

（2）TiO_2 for inorganic removal

TiO_2 nanoparticles could be used to adsorb phosphates under UV irradiation, as supported in Xie et al.'s study[36]. 95% of total phosphates was removed from surface water within 10 min. Similarly, Shavisi et al. removed ammonia by a floating TiO_2 system (immobilizing TiO_2 nanoparticles with expanded clay aggregate granules) under solar light[35]. Differences were noted on the fact that the effects of pH varied in ammonia and phosphorous removal. Also, N,N'-ethylenediamine-disuccinic acid and copper ions could be oxidized 100% in TiO_2 photocatalytic reaction[31].

（3）TiO_2 for microbial removal

It is well recognized that TiO_2 is capable of disinfection through photocatalytic reaction, which is ascribed to two major oxidants (OH radical and ROS). Cho et al. investigated the mechanism of biocidal action of TiO_2 and found that the inactivation rate of E.coli was linearly correlated to the concentration of OH radicals[41]. Besides, a wealth of research has been carried out to better understand the disinfection process. Mutsunaga et al. firstly used Pt/TiO_2 to kill *E.coli* and obtained good photochemical sterilization results[42]. Maness et al. detected 77-93% losses of the cell respiratory activity in the presence of TiO_2 under near-UV light and concluded that the strong bactericidal activity was due to the promotion of peroxidation of the polyunsaturated phospholipid component in the membrane by TiO_2[43].

Furthermore, in the presence of ferrous ions at low concentration, the inactivation activity of TiO_2 could be enhanced by 200%, as reported by Sjogren and Sierka[44]. This was attributed to the increase of OH radical due to Fenton reaction. Benabbou et al. also investigated the effect of TiO_2 concentration and intensity of UV irradiation on the photocatalytic inactivation of *E.coli*[45]. Results showed that the disinfection was enhanced with increasing light intensity from UVA to UVC, and the optimum TiO_2 concentration was 0.25 g/L. However, in Min et al. and Pulgarin et al.'s studies, higher efficiency was detected in higher TiO_2 concentration, contrary to Benabbou et al.'s findings[46, 47]. That may be attributed to the different *E.coli* concentrations and lights used in their specific experiments.

2.3 TiO_2 modification

There are many approaches for TiO_2's modification, including coating organic dyes, doping with metal ions, heavy metal precipitation, size modification, system modification and so on. Figure 2 illustrated three main methods in details. Organic dyes and heavy metal could help electrons transfer, and metal ions narrowed the band gap.

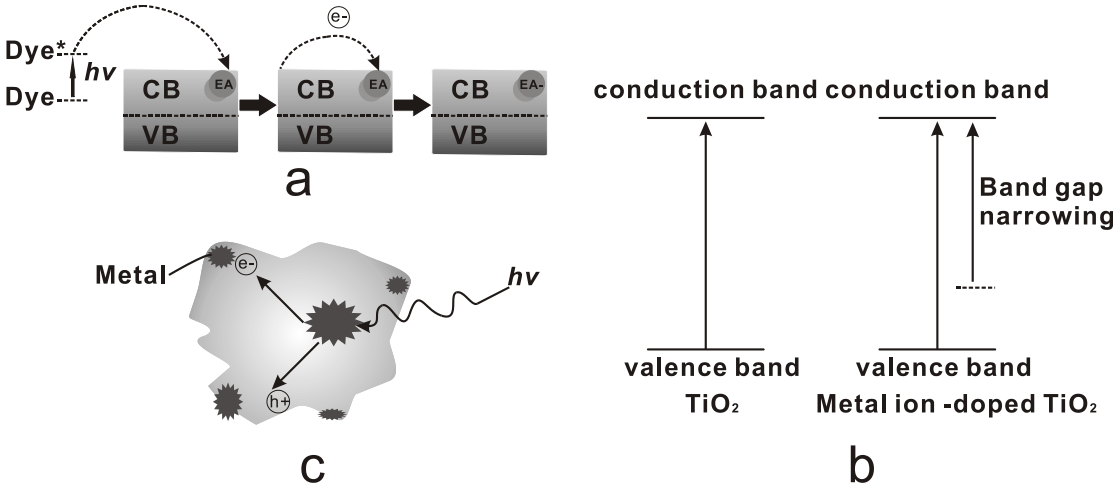

Figure 2. Approaches for TiO_2 modifications: (a) coating organic dyes, (b) doping with metal ions and (c) heavy metal precipitation.

Many researchers have focused their attention on the modification of TiO_2. Song et al. prepared PVA/TiO_2 composite films by thermal treatment and extended its available absorption wavelength from UV to visible region[48]. Unsaturated polymer acted as organic dyes and transferred photoinduced electrons to TiO_2. Films with 180 ℃ treatment degraded RhB solution to 11% in 6 h and showed relatively better performance.

Badawy et al. fabricated Ag/TiO_2 nanoparticles at room temperature and received good removal efficiency for pharmaceutical pollutants[34]. Li et al. synthesized N-F-codoped TiO_2 nanoparticles by spray pyrolysis and claimed that this kind of photocatalyst could have extended absorption wavelength from UV to visible range (<550 nm)[49]. Here, F element could introduce new active sites, while N element played a role in visible absorption. Wang et al. chose sulfate to modify TiO_2 and observed more strong Lewis and Bronsted acidic sites on the surface of particles that led to higher photocatalytic performance[50].

TiO_2 could also be modified by combining the advantages of metal and inorganic elements. Du and Yu synthesized Zr-N-TiO_2 nanoparticles by sol-gel method. This kind of photocatalyst had a narrower band gap and its absorption range red-shifted to visible region through replacing Ti with Zr and O with N, respectively[33].

2.4 System modification

In traditional wastewater treatment, TiO_2 nanoparticles were generally used in slurry systems for sake of large surface area. However, the recycling of TiO_2 has been a tricky problem for its application. Improper recycling process would led to mass loss, or even secondary pollution as a consequence. Therefore, in order to solve this problem, many researchers have devoted their efforts to the immobilization of TiO_2 by various methods.

TiO_2 nanoparticles could be fixed on different substrates, such as glass slides, steel plate, polymer and so on. In Gelover et al.'s study, TiO_2 and glass pieces were connected together to avoid post-separation process[51]. Kieda and Tokuhisa uniformly deposited TiO_2 nanoparticles on metal substrates electrolytically[52]. Zeng et al. prepared a kind of portable composite films by fixing TiO_2 onto cellulose via sol-gel method and these films could remove phenol at a high rate[53]. Lei et al. immobilized TiO_2 in PVA matrix by forming Ti-O-C chemical bond through solution-casting and heat-treatment method[54]. They have found that, even after 25 cycles, these films could still remain stable with only slight mass loss.

Besides these, changing the shape of TiO_2 was also another interesting approach. Ng et al. synthesized a nanofungus-like TiO_2 film, which in result brought benefit to post-separation[55]. Pang et al. mentioned TiO_2-based nanotubes and summarized the progress of one-dimensional TiO_2 nanotubes in detail[56]. Because of the extended length, TiO_2 nanotubes could be excluded outside of the biopolymers and be recycled easily. For instance, in Zhang et al.'s study, 10 nm TiO_2 nanowire was combined with microfiltration and showed complete reclamation and better photocatalytic activity than P25. Even larger size of 20 nm TiO_2 nanowires still had the same photocatalytic efficiency as P25[57]. Sun et al., on the other hand, tried to fabricate porous TiO_2 microsphere and applied it in membrane reactor[58]. In this designed system, 70% of phenol could be removed within 60 min under UV light irradiation.

2.5 Transparency property

Even though the performance of TiO_2 has been greatly improved, the opaque colored and powdery properties still inhibited its application in buildings and other relevant fields. For the modification of TiO_2's transparency property, various methods has been used.

According to previous research, the optical property of TiO_2 could be improved by silica coating with higher UV adsorption[59]. Besides, C-N-F-codoped TiO_2 films were also observed to be transparent and visible light driven for self-cleaning applications[60].

On the other hand, transparent polymer has been a hot topic for the modification of TiO_2's optical property. Subianto et al. evenly distributed TiO_2 on plastic fibers using wet polyurethane as a linking material[61]. Liu et al. connected transparent PVA with TiO_2 and obtained hybrid films with enhanced photocatalytic activity and good stability[62]. Antonello et al. synthesized transparent TiO_2 films by electrical deposition[63]. Ahmadpoor et al. prepared transparent PVA/TiO_2 fibers by electrospinning technique[64].

Chapter 3 MATERIALS AND METHODS

3.1 Chemicals and materials

P25 (aeroxide TiO_2, hydrophilic) and PVA (average molecular weight 10,000, cold water soluble) were purchased from Sigma-Aldrich (St. Louis, MO). P25 is a fluffy white powder with average primary particle size of 21 nm. Its specific surface area was 50 ± 15 m^2/g. The pH value of its aqueous solution ranged between 3.5 and 4.5.

Sodium chloride (NaCl, ≥99.5%), ethanol (96% volume ratio) were ordered from VWR (Singapore). MB and RhB was purchased from Sigma-Aldrich (St. Louis, MO) and used as the model pollutant during photocatalytic reaction. All chemicals were used without any further purification and DI water from an ELGA PURELAB Option System with a resistivity of $\geqslant 18.2$ MΩ cm^{-1} was used to prepare aqueous solutions.

3.2 Preparation of the P25/PVA hybrid films

Films were prepared according to the flow chart depicted in Figure 3 and details are described in the followings. After weighing certain amount of PVA and P25, the two powders were dissolved into 15 mL DI water and marked as solution A and B, respectively. For sake of good dissolution and dispersion result, solution A need to be stirred at 350 rpm and 90 ℃ for 1 h, while solution B stirred at room temperature for 30 min after 30 min of sonication pretreatment. Subsequently, these above two

solutions were mixed together (thus giving total solution volume of 30 mL) and transferred into a 40 mL Teflon-lined autoclave. The mixture in autoclave was then treated at 150 ℃ in an oven for 3 h. After cooling down to room temperature, the final solution could be used to prepare hybrid films by drop casting certain amounts of solution (this is denoted as the dropcast volume in later discussion) onto clean and blank glass slides. Finally, thermal treatment of these hybrid films were performed at different temperatures for comparison.

3.3 Methodology

（1）Chemical test

MB was used as a typical organic pollutant to evaluate the photocatalytic activity of P25/PVA hybrid films. In each set of experiment, one piece of hybrid film (2x2 cm) was put in 30 mL MB solution at the concentration of 10 mg/L and stirred in the dark for 1 h before taking the first absorption measurement (C_0). The solution with catalyst was then irradiated under simulated solar light (Solar simulator, sun 2000, AVET technologies) inside a water-cooled beaker. Samples were taken from the reactors every 20 min for the duration of 2 h for analysis.

Prior to chemical quantification, the collected liquid samples were centrifuged at 12,000 rpm for 2 min to remove the dislodged TiO_2 particles from the film. Absorption spectrum was then scanned from 300 nm to 800 nm. The maximum

absorption wavelength for MB observed at 662 nm was monitored. Other typical pollutant, RhB, was also studied with similar procedures.

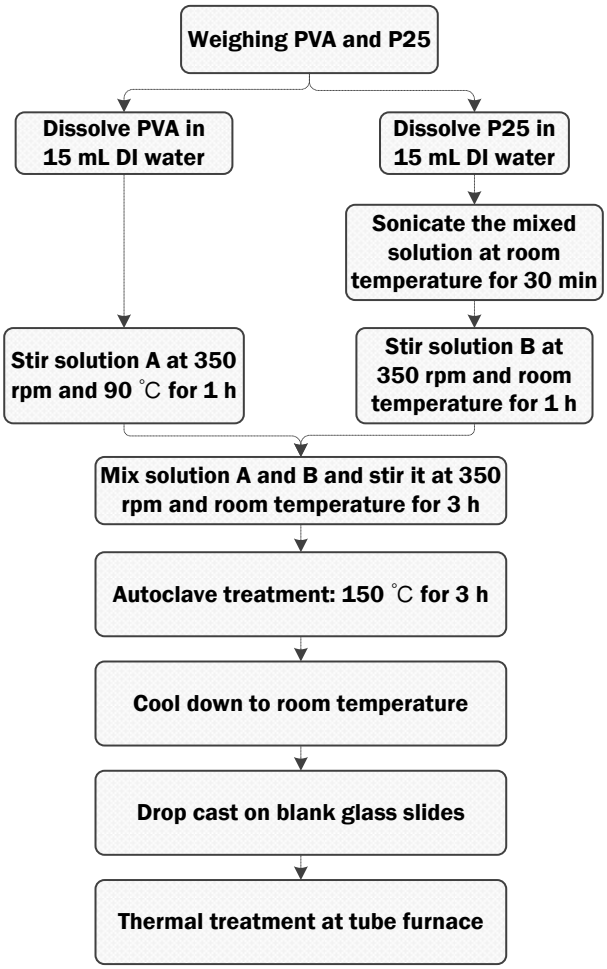

Figure 3. Flow chart for the synthesis procedures of TiO_2/PVA films.

（2）Microbial test

E.coli K12 (gram-negative) was used as a representative to evaluate the anti-bacterial activities of the synthesized films. Steps were referred to Tian et al.'s experiment[30]. First of all, *E.coli* K12 was incubated in LB nutrient solution at 37 ℃ for 24 h with continuous shaking. Subsequently, the solution was washed and diluted

in gradient with 0.9% saline. Then, 0.3 mL of the diluted solution and 30 mg hybrid films were used for photocatalytic reaction in 30 mL saline. Finally, samples were collected every 15 minutes and the remaining number of *E.coli* K12 was measured by by LB agar plates incubation. At the same time, similar setup without the hybrid film was also conducted as a control.

（3）Mechanical test

Mechanical test was conducted by stirring process with varying stirring rate and time length. Mass changes were recorded before and after the stirring process. The difference in mass indicated the stability of the hybrid films.

3.4 Instrumentation

All of the instruments used in this experiment were shown in Table 2, as followed.

Table 2. A list of instruments used in this experiment.

Index	Instrument
UV-VIS	UV-3600, SHIMADZU, UV-VIS-NIR spectrophotometer
Light	Solar simulator, sun 2000, AVET technologies
Centrifugation	Profuge 14k
Microscope figures	SOP for Nikon Eclipse LV100D, microscope
Stirrer	Fisher scientific
Weight	GR-200
Sonication	ελma, E30H, Elmasonic, 220-240 V/AC, 50/60 HZ, 240 w
Oven	MEMMERT, P.O.Box 1720
FT-IR	Varian 3100 Excalibur Series, 4000 to 400, scanning range 16, Resolution 4 cm-1, KBr was used for sample preparation
Tube furnace	Carbolite, TZF 12/38/400, 220-240 V, 1280 W, AMPS MAX: 5.4
SEM	JEOL JSM-6700F Field Emission Scanning Electron Microscope

Chapter 4 OPTIMIZATION OF P25/PVA HYBRID FILMS

4.1 Optimization of the curing temperature

According to previous research, thermal treatment could be used to achieve film stabilization[48]. However, insufficient or too high temperature might affect or even do harm to the final films. Therefore, proper control of the curing temperature would be a critical parameter for the final performance of the hybrid films. As shown in Table 3, four sets of experiments were carried out in this project with varying temperature treatment.

Table 3. Preparation parameters of hybrid films treated at different temperatures.

Sample	PVA	P25	Ratio	Solution volume	Film thickness*	Curing temperature
1-1	0.125 g	0.125 g	1:1	30 mL	0.25 mL	120℃
1-2	0.125 g	0.125 g	1:1	30 mL	0.25 mL	150℃
1-3	0.125 g	0.125 g	1:1	30 mL	0.25 mL	180℃
1-4	0.125 g	0.125 g	1:1	30 mL	0.25 mL	210℃

*: Film thickness was controlled by the dropcast volume of cast solution.

(1) Color of the resultant films

During this experiment, the change of films' color was visually inspected.

Results showed that with the increase of curing temperature, hybrid films gradually changed their color from white to yellow and brown, similar to Song's observation[48].

For films treated at 120 ℃and 150 ℃, the color of final films appeared nearly the same, i.e. they remained white during the whole process. But when the film was heated to 180 ℃, some parts of the film began to change their color to yellow and even darker color. At even higher temperature of 210 ℃, remarkable changes could be detected and the hybrid films became brown and not-transparent. This observation indicated that the basic compositions of P25/PVA films had been transformed into other components at this high temperature.

(2) Transparency property of the resultant films

Corresponding to color change, the transparency property of the hybrid films was also affected by the various temperature treatment (Figure 4). Films treated at 120 ℃ had the highest transmittance in the whole wavelength range, while higher temperature contributed to worsen transparency property. All hybrid films showed lower transmittance when the wavelength was below 350 nm, similar to previous research[48].

The differences of light transmittance for films treated at 150 ℃ and 180 ℃ mainly occurred in the range of 350-550 nm. Only small decrease could be observed in longer wavelengths. But for films treated at 210 ℃, the decrease was very obvious in all wavelengths ranging from short to long wavelengths.

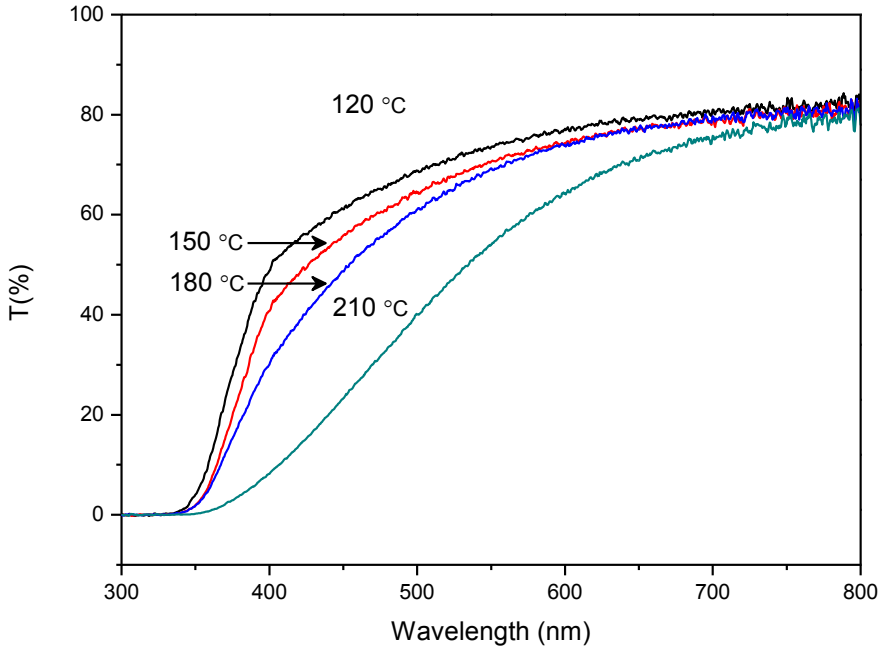

Figure 4. The transparency property of hybrid films treated at different temperatures measured as its transmission over the range of 300-800 nm.

(3) Photocatalytic efficiency

The decay of MB via solar irradiation catalyzed by films with different temperature treatment was investigated. All of the decays were found to follow pseudo-first order kinetics. As shown in Figure 5, films treated at 150 ℃ has the highest photocatalytic efficiency. Within 120 min, 10 mg/L MB had been degraded down to about 20% and the film showed good stability during the whole reaction. The worst photocatalytic effect was detected for films treated at 210 ℃; only 30% of MB could be degraded under the same irradiation conditions. For the other two samples, the film treated at 120 ℃ benefited more when compared with that at 180 ℃. It might be due to the worse transparency property and change of materials under excess

high temperature. Wang et al. explained that overly high temperature would transform PVA to layers of carbon that cover the surface of the photocatalyst. P25, on the other hand, could become larger in size during heat treatment, which in result reduced its surface area and the opportunity to contact with pollutants[65]. Therefore, conclusions could be made that 150 ℃ should be a better curing temperature for the hybrid films.

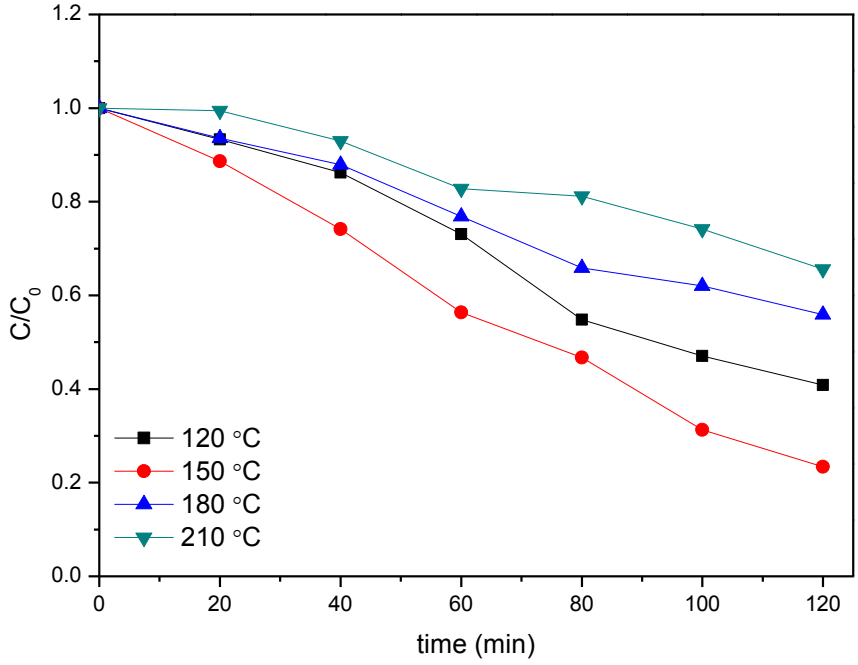

Figure 5. The photocatalytic efficiency of hybrid films treated at different temperatures.

(4) IR and morphological changes of the hybrid films treated at different temperatures

For better understanding of the effects of curing temperature, FT-IR spectroscopy and optical microscopy were used to measure the changes of functional groups and microstructure of the final films. As could be seen in Figure 6, large differences mainly occurred in wavenumber around 500 cm^{-1} (Ti-O vibration, enhanced by PVA

addition, which indicates the interaction between P25 and PVA[21]), 1144 cm^{-1} (C-C stretching, the crystallization-sensitive bond[66]), 1250 cm^{-1} (C-H wagging[21]), 1668 cm^{-1} (dehydration of PVA and formation of C=C double bonds[67]), 1720 cm^{-1} (C=O stretching, indicating the oxidation of PVA molecules[66]) and 2820 cm^{-1} (C-H vibration[66]). This indicated that as temperature increased from 120 ℃ to 210 ℃, C-OH could be gradually oxidized into C=O and the linkage of PVA and P25 became much stronger. The formation of C=O group and layers of carbon mentioned above, acting as chromophore, absorbed light in visible and near IR region[66]. Consequently, dark color appeared in the surface of hybrid films with high thermal treatment. As reported by Ahmad et al., C= O and C=C were observed around 208 nm in UV-vis absorption spectrum[21].

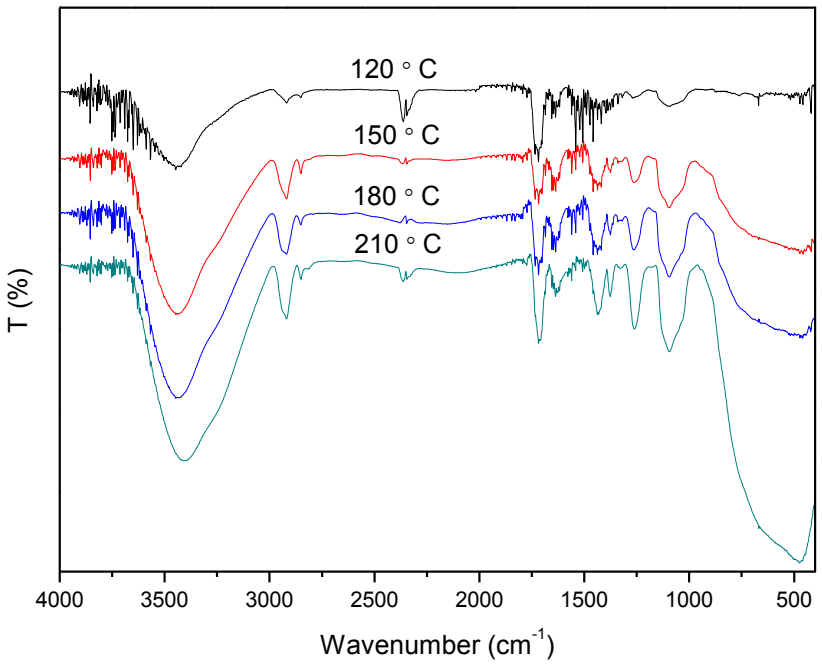

Figure 6. FT-IR spectra of hybrid films treated at different temperatures.

Microscopic images also showed some differences among the various samples (Figure 7). Films treated at higher temperatures had relatively coarse surface and apparent cracks. According to Song et al.'s experiment, thermal treatment would not affect the distribution of P25, but brought about some microcracks on the surface of the films. Proper heat treatment would increase the specific area of the photocatalyst and promote the photocatalytic activity[48]. Therefore, this observation was mainly attributed to the degradation of PVA under high thermal treatment.

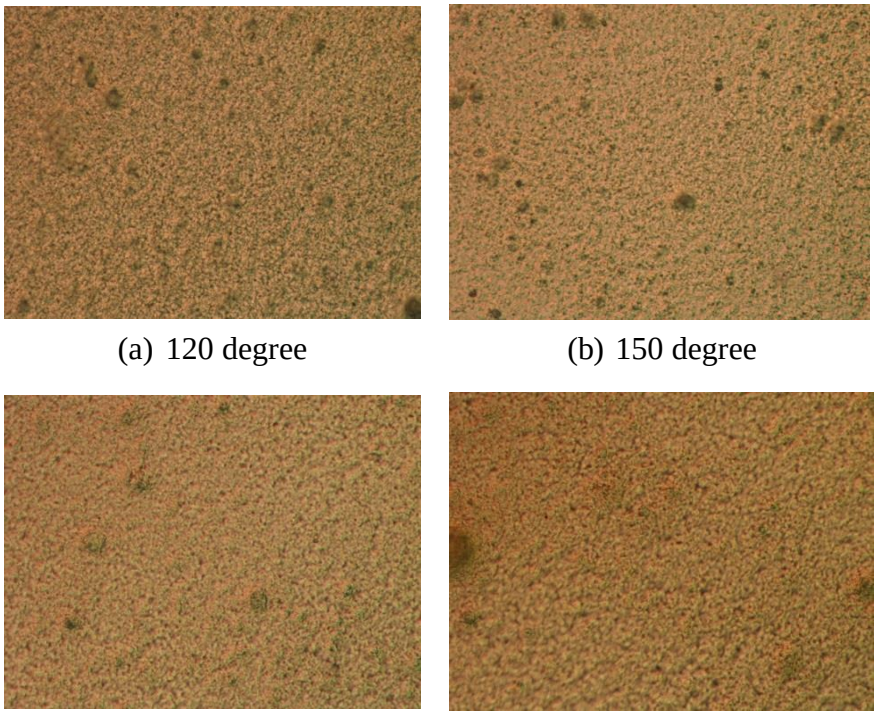

(a) 120 degree (b) 150 degree

(c) 180 degree (d) 210 degree

Figure 7. Microscopic images of hybrid films treated at different temperatures: (a) 120 ℃, (b) 150 ℃, (c) 180 ℃ and (d) 210 ℃. (Magnification was the same as that shown in other microscopic images of the following text)

(5) Control experiment using pure PVA cast films

According to the above findings, the effect of curing temperature on

photocatalytic efficiency is significant. In this section, we investigated pure PVA cast films subjected to the same temperature treatment in order to figure out if PVA is the dominant component that affect the hybrid films.

Results from transparency test (Figure 8) and FT-IR spectra (Figure 9) of pure PVA films showed similar trends as the hybrid films, with the exception of the absorption peak at 840 cm^{-1} (the vibration of C=C in R-CH=CH_2[21]). Thus, temperature treatment darkened its color, decreased its transparency property and enhanced the formation of C=O. The effect is especially significant for films treated at 210 ℃. Hence, it seems that changes of the hybrid films are mainly due to changes in the PVA component of the films.

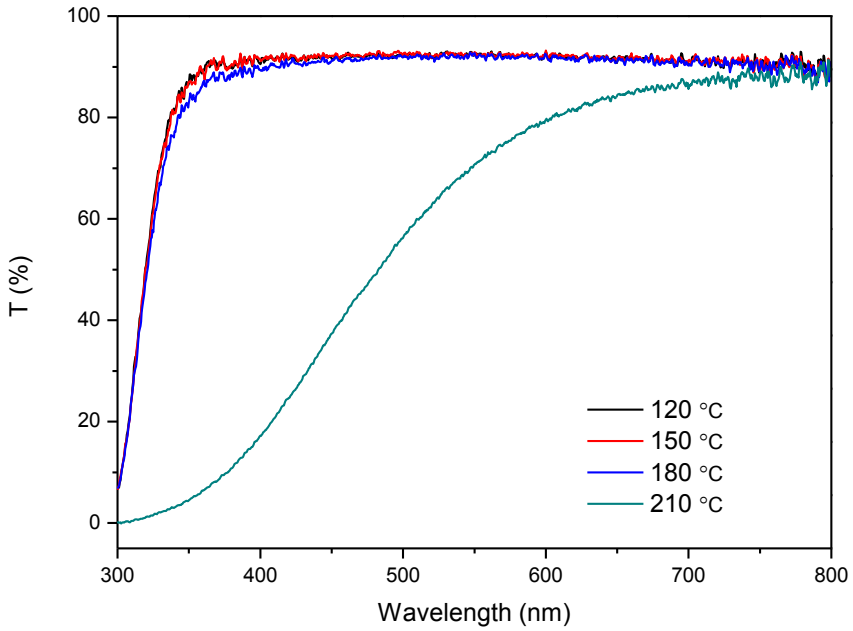

Figure 8. The transparency property of pure PVA films treated at different temperatures measured as transmission over the range of 300-800 nm.

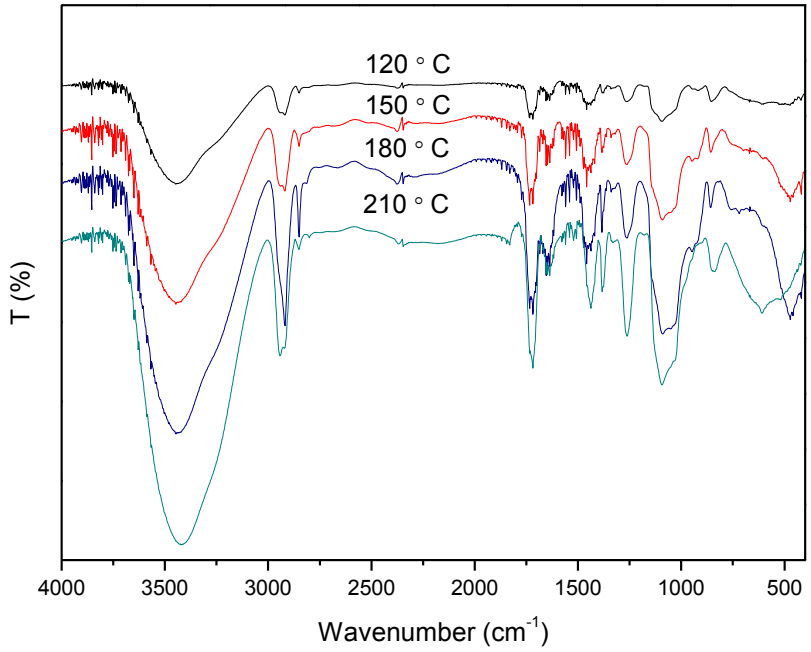

Figure 9. FT-IR spectra of pure PVA films treated at different temperatures.

However, slight differences in transparency property are still observed comparing with the hybrid films. Pure PVA films treated with 150 ℃ and 180 ℃ showed comparatively less attenuation in transparency than the corresponding hybrid films. We believe this can be explained by the existence of P25 particles in the hybrid films. P25 nanoparticles was much easier to coagulate into bigger sizes under high thermal environment, which would thus scatter more light from the surface. Thus, the combined effect of larger sizes and less active sites of the catalyst would have caused the differences in photocatalytic efficiency of these films.

4.2 Optimization of film thickness

Besides curing temperature, film thickness was also another important parameter to consider. Tada and Tanaka studied the effects of film thickness on photocatalytic activity and found that appropriate film thickness could well balance transparency property and photocatalytic activity [68].

In this project, the thickness of the hybrid films was controlled by the dropcast volume of the cast solution, which was varied from 0.125 mL to 0.75 mL. Detailed parameters were listed in Table 4.

Table 4. Preparation parameters of hybrid films with different film thickness.

Sample	PVA	P25	Ratio	Solution volume	Film thickness*	Curing temperature
2-1	0.125 g	0.125 g	1:1	30 mL	0.125 mL	150℃
2-2	0.125 g	0.125 g	1:1	30 mL	0.25 mL	150℃
2-3	0.125 g	0.125 g	1:1	30 mL	0.50 mL	150℃
2-4	0.125 g	0.125 g	1:1	30 mL	0.75 mL	150℃

*: Film thickness was controlled by the dropcast volume of cast solution.

(1) Transparency property of the resultant films

According expected, with the increase of drop amounts, the transparency property of the hybrid films decreased gradually. As shown in Figure 10, the film with

0.125 mL drop volume could transmit more than 30% light than that with 0.75 mL. Yu et al. believed that this decrease was attributed to the increase of opacity and light scattering in thick films[69].

Besides these, it was interesting to note that the gaps between each spectra line was quite similar. That, to some aspect, suggested that the film thickness affected on the film superficially, but did not bring about other significantly inner changes.

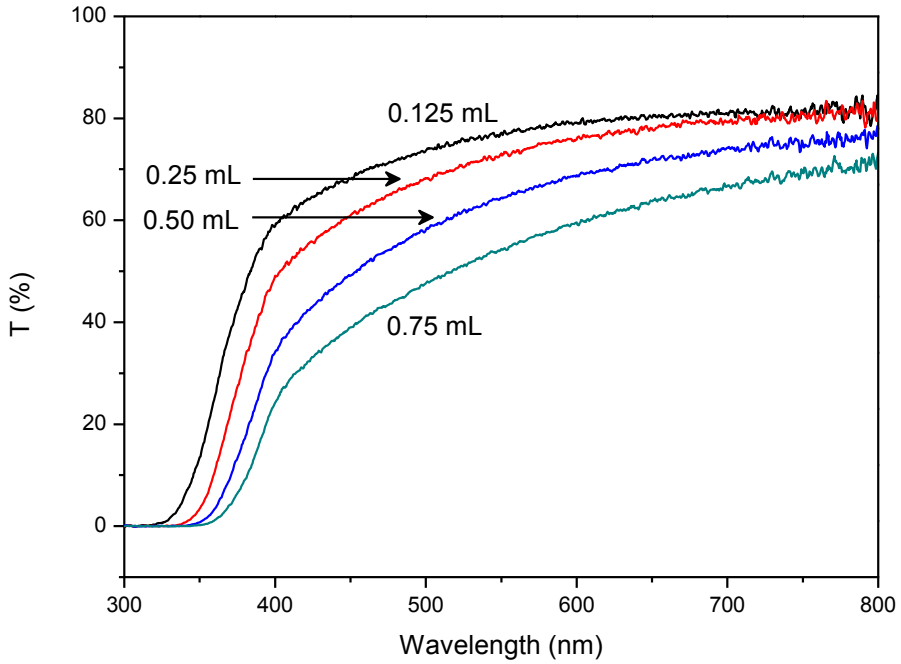

Figure 10. The transparency property of hybrid films with different film thickness.

(2) IR and morphological changes of the hybrid films with different film thickness

Similar conclusions could also be made from FT-IR spectra (Figure 11) and microscopic images (Figure 12). Differences among the hybrid films with various film thickness was insignificant when the drop volume ranged from 0.125 mL to 0.75

mL. There were nearly no changes of functional groups and microstructures for films with different thickness.

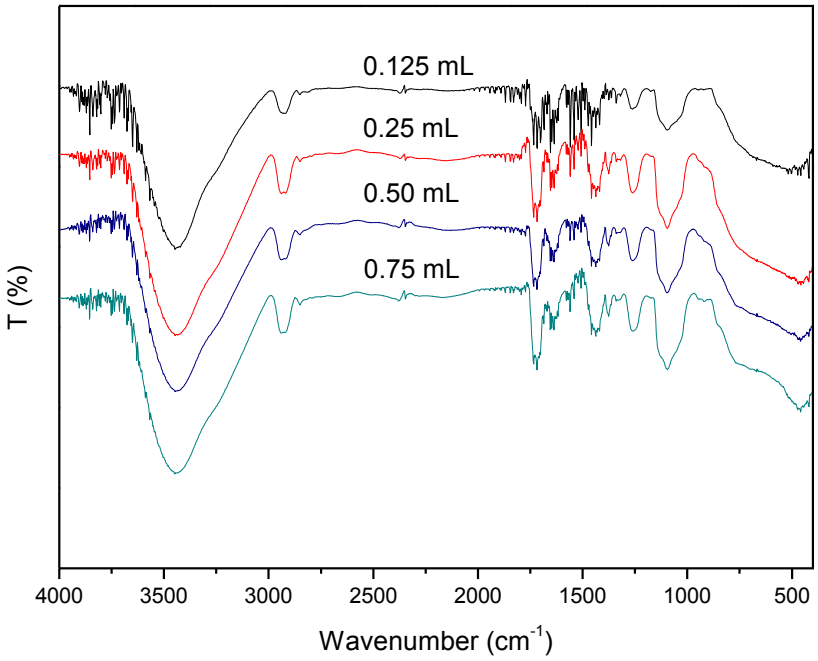

Figure 11. FT-IR spectra of the hybrid films with different film thickness.

(3) The photocatalytic efficiency and mass changes of hybrid films with different film thickness

Even though there are no significant changes detected in the morphology and IR spectrum among the hybrid films with different film thickness, the photocatalytic activity was found to vary along the series of samples (Figure 13). The hybrid film with 0.25 mL drop volume could degrade 10 mg/L MB solution at the highest rate, whereas those with 0.75 mL and 0.50 mL drop volumes showed the worst performance. Only 30% of MB could be degraded after 120 min of the photocatalytic reaction. This phenomenon indicated that the drop volume for the 2x2 cm glass slides

should not be more than 0.50 mL.

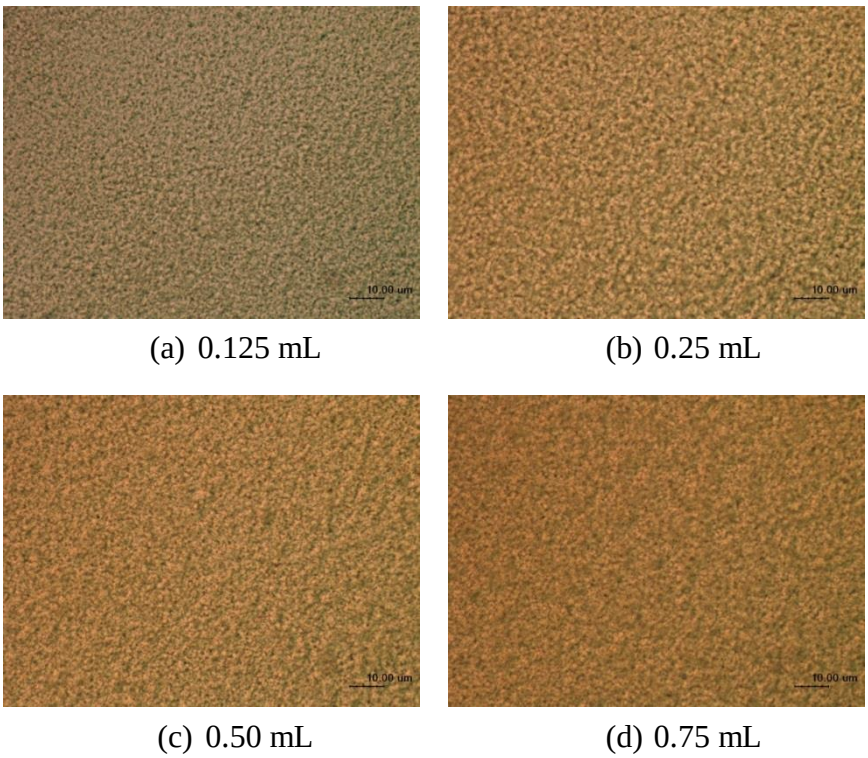

(a) 0.125 mL (b) 0.25 mL

(c) 0.50 mL (d) 0.75 mL

Figure 12. Microscopic images of hybrid films with different film thickness: (a) 0.125 mL, (b) 0.25 mL, (c) 0.5 mL and (d) 0.75 mL.

We found that too much drop volume would affect the formation of stable film and thus cause large mass changes before and after the photocatalytic study as listed in Table 5. The mass loss of film with 0.75 mL drop volume was 2 times as that of the film with 0.5 mL drop volume, and more than 13 times as that of the film with 0.125 mL drop volume. This observation confirms that increasing drop volume does not necessarily gives rise to more photocatalyst for the reaction. In addition, the excess photocatalyst will not bind strongly to the glass surface and will be dislodged by the stirred solution[69].

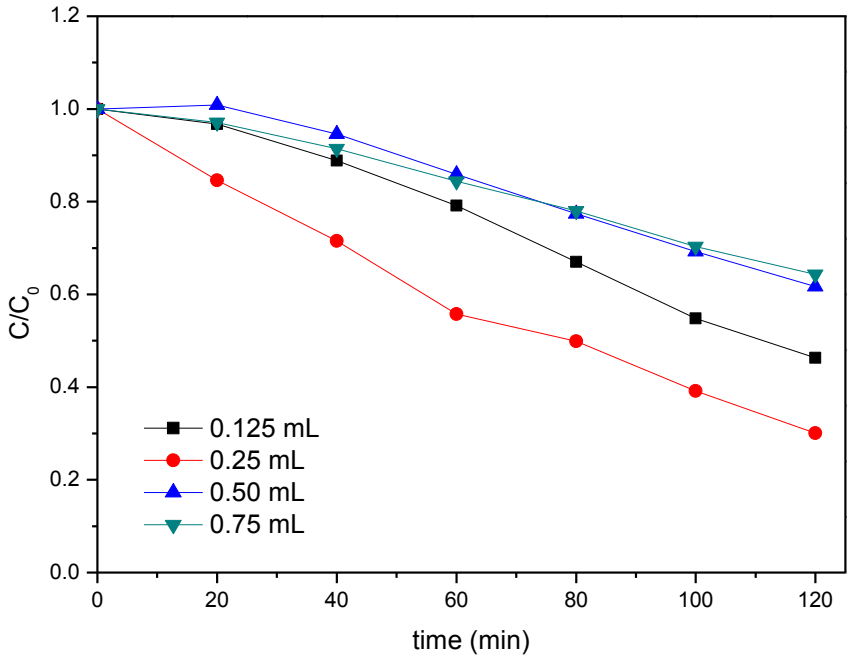

Figure 13. The photocatalytic efficiency of hybrid films with different film thickness.

Table 5. Mass changes of hybrid films with different film thickness before and after the photocatalytic reaction.

Samples	Mass (g)		
	Before experiment	After experiment	Difference
0.125 mL	1.1755	1.1752	0.0003
0.25 mL	1.0374	1.0362	0.0012
0.5 mL	1.1207	1.1187	0.0020
0.75 mL	1.0465	1.0425	0.0040

On the other hand, if the drop volume was not insufficient, the photocatalytic

activity would be reduced due to the lack of active sites, such as that observed for the hybrid film with 0.125 mL drop volume. Therefore, proper film thickness should be casted by 0.25 mL solution onto 2x2 cm area. According to Chen et al.'s research, pure TiO_2 films with the thickness of 10 μm performed best without forming cracks[70]. By the addition of PVA, films thickness should be further measured in future research.

4.3 Optimization of the feed ratio of P25/PVA

On the basis of optimum curing temperature and film thickness, we attempt next to optimize the feed ratio of P25/PVA. In this section, the mass of P25 was set constant as 0.125 g. By changing the amount of PVA, P25/PVA ratio was varied from 2:1 to 1:4. Detailed information was listed in Table 6.

Table 6. Preparation parameters of hybrid films with different feed ratio of P25/PVA.

Sample	PVA	P25	Ratio	Solution volume	Film thickness*	Curing temperature
3-1	0.0625 g	0.125 g	2:1	30 mL	0.25 mL	150℃
3-2	0.125 g	0.125 g	1:1	30 mL	0.25 mL	150℃
3-3	0.250 g	0.125 g	1:2	30 mL	0.25 mL	150℃
3-4	0.500 g	0.125 g	1:4	30 mL	0.25 mL	150℃

*: Film thickness was controlled by the dropcast volume of cast solution.

(1) Transparency property and morphological changes of the hybrid films with different feed ratio of P25/PVA

Different feed ratio of P25/PVA led to different distribution of microstructures on the hybrid films. As shown in Figure 14, with increasing PVA addition, hybrid films began to be dominated by PVA instead of P25 and the hybrid films correspondingly changed their color gradually from dark to lighter color in microscopic images (Figure 14).

Furthermore, the films with 1:2 and 1:4 feed ratio seemed to be more homogeneous than those with 2:1 and 1:1 feed ratio.

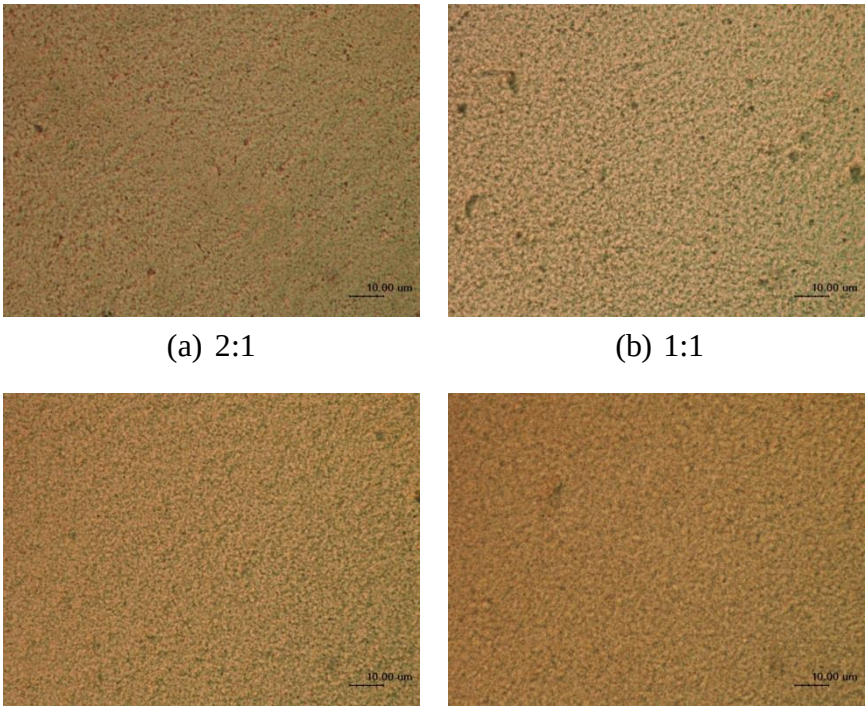

(a) 2:1 (b) 1:1

(c) 1:2 (d) 1:4

Figure 14. Microscopic images of hybrid films with different P25/PVA ratio: (a) 2:1, (b) 1:1, (c) 1:2 and (d) 1:4.

We have found also that, after thermal treatment, the hybrid films with various P25/PVA feed ratio showed different colors. The more PVA was added, the darker the color of the hybrid films. The films with the 2:1 and 1:1 feed ratios did not change their color significantly, while films with 1:2 and 1:4 feed ratios turned yellow and brown, which suggested that PVA was more easily affected by the thermal treatment.

The hybrid films with more PVA also showed less transmittance, as illustrated in the transparency spectra (Figure 15). Comparing with the hybrid film with 1:1 feed ratio, that with 1:2 feed ratio decreased its transmittance from 300 nm to 600 nm. The wavelength of yellow light was around 580 nm. This observation agreed well with the color change of this hybrid film from feed ratio 1:1 to 1:2.

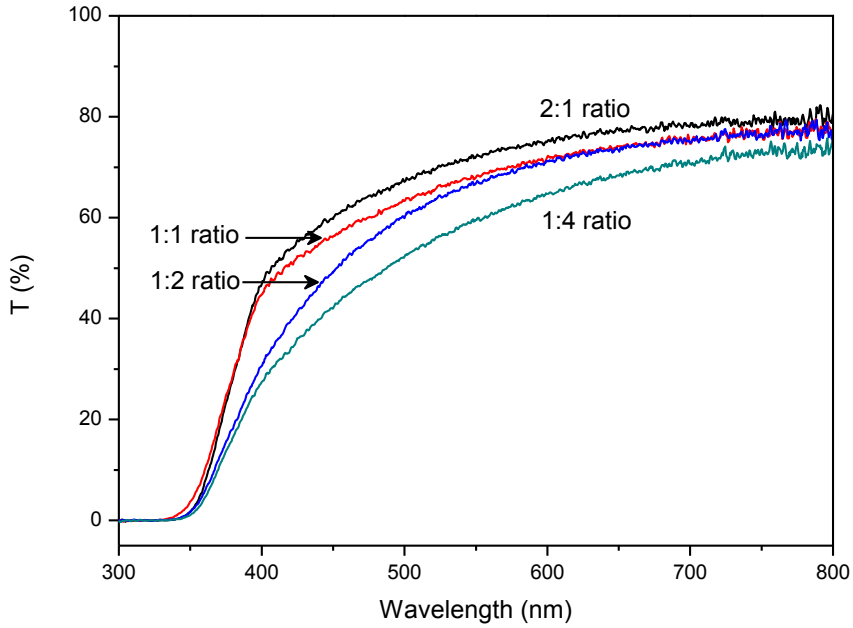

Figure 15. The transparency property of hybrid films with different P25/PVA ratio.

Besides, P25 is known to be a white powder with strong absorption in UV range. As shown in Figure 15, P25/PVA hybrid films could conserve the property of TiO_2 well, even in low doping film, cutting off UV transmission. Similar results were also reported in Ahmad et al.'s research[21].

(2) IR spectra of the resultant films

The feed ratio of P25/PVA affected the IR spectra significantly, as illustrated in Figure 16. Major differences occurred in wavenumber around 500 cm^{-1} (Ti-O vibration, enhanced by PVA addition, which indicates the interaction between P25 and PVA[21]), 1250 cm^{-1} (C-H wagging[21]), 1720 cm^{-1} (C=O stretching, indicating the oxidation of PVA molecules[66]) and 2820 cm^{-1} (C-H vibration[66]). After a initial increasing trend, the hybrid films began to gradually decrease their transmittance intensity at 500 cm^{-1} as more PVA was added. The hybrid film with 1:1 feed ratio showed the strongest absorption peak, which reflected the strongest linkage between P25 and PVA. Excess PVA addition reduced this relationship.

A schematic diagram showing the chemical linkage between PVA and P25 is given in Figure 17, as explained in Maurya et al.'s report[71]. Similar trend was also observed in other peaks, which indicated the enhanced vibration of PVA and the formation of C=O in the hybrid film with 1:1 feed ratio. Thus, the optimal feed ratio of P25/PVA was found to be 1:1 from this study.

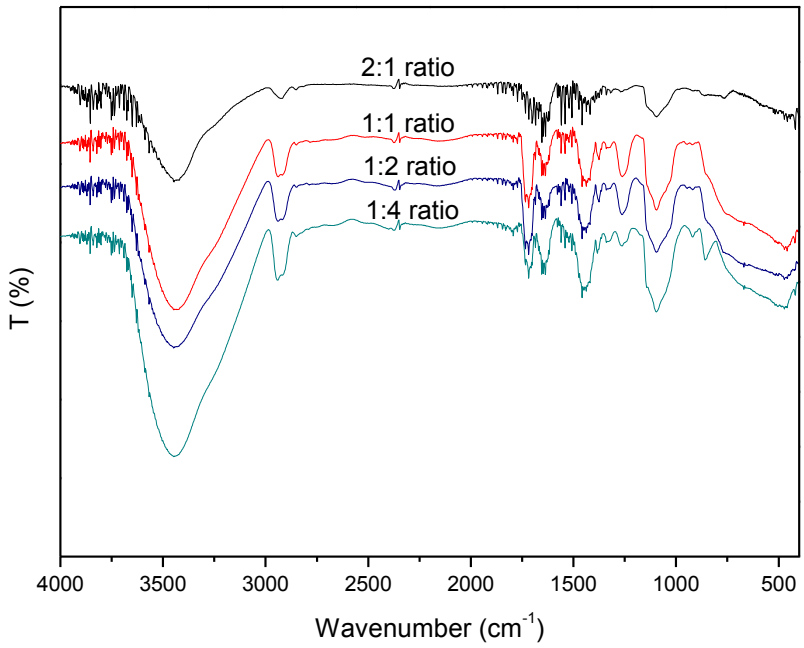

Figure 16. FT-IR spectra of hybrid films with different P25/PVA ratio.

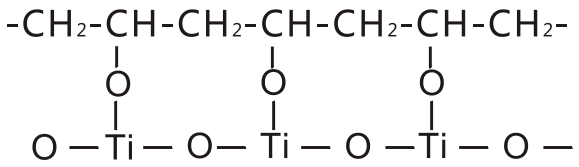

Figure 17. Schematic diagram showing the chemical linkage between P25 and PVA.

(3) Photocatalytic efficiency and stability of the resultant films

It was interesting to note that different P25/PVA ratio could alter photocatalytic reaction to different degrees (Figure 18). Except the hybrid film with 2:1 ratio, all the other films performed well during the photocatalytic reaction. Within 120 min, the original concentration of MB could be reduced by 80%.

There were several proposals on the role of PVA in P25/PVA hybrid films.

During the thermal treatment process, PVA could be partly degraded into unsaturated PVA (named as H-PVA). This H-PVA acted as organic dyes that could transfer electrons to P25, thus result in enhanced photocatalytic activity[65]. However, on the other hand, the addition of PVA would reduce the surface area of exposed P25 and the transparency of the film[48]. Thus, a balance between the surface area of exposed P25 and the amount of H-PVA need to be obtained. Only proper feed ratio of P25/PVA could well balance these two aspects and provide better performance.

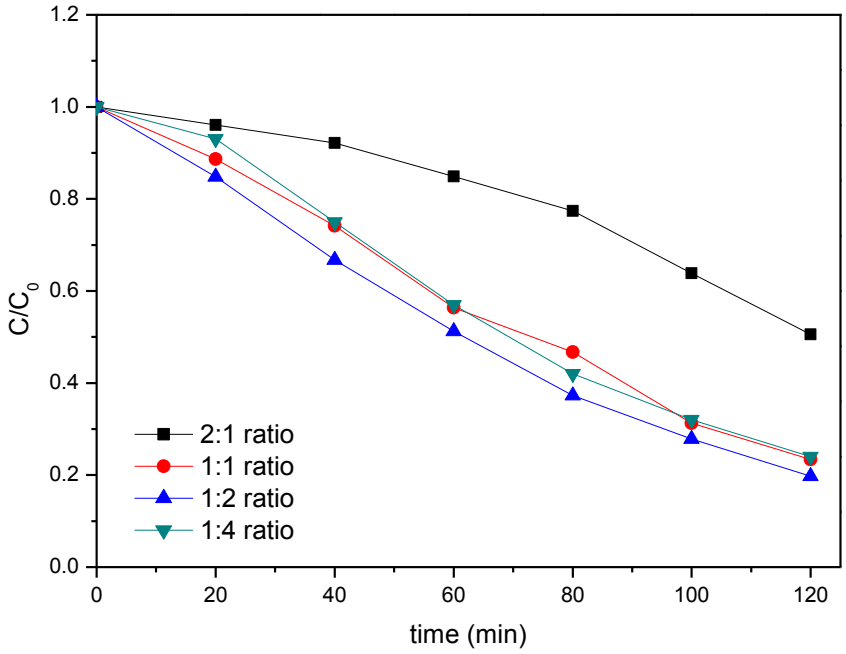

Figure 18. The photocatalytic efficiency of hybrid films with different P25/PVA ratio.

Interestingly, the mass loss values in Table 7 suggest that the mechanical properties of the hybrid films were not enhanced by more PVA addition[21]. The hybrid films with 1:1 and 1:2 feed ratio showed relatively better mechanical stability.

Kadem et al. also obtained this result by ultrasonic tests[72]. It was proposed that the addition of TiO_2 occupied the vacancies between PVA molecules and maintained good mechanical property of the hybrid films.

Table 7. Mass changes of hybrid films with different P25/PVA ratio before and after the photocatalytic reaction.

Samples	Mass (g)		
	Before experiment	After experiment	Difference
2:1	1.1310	1.1306	0.0004
1:1	1.1642	1.1632	0.0010
1:2	1.1585	1.1565	0.0020
1:4	1.1529	1.1507	0.0022

(4) Stability test

Good photocatalytic activity and stable property were important for films' application. The stability of the photocatalyst, on the other hand, is also an important performance parameter. Thus, we repeat the photocatalysis studies by 3 cycles using films with 1:1 and 1:2 feed ratio in this section. Results indicated that the photocatalytic performance of the hybrid film with 1:1 ratio is repeatable within these three cycles with only slight loss in efficiency (Figure 19 and Table 8).

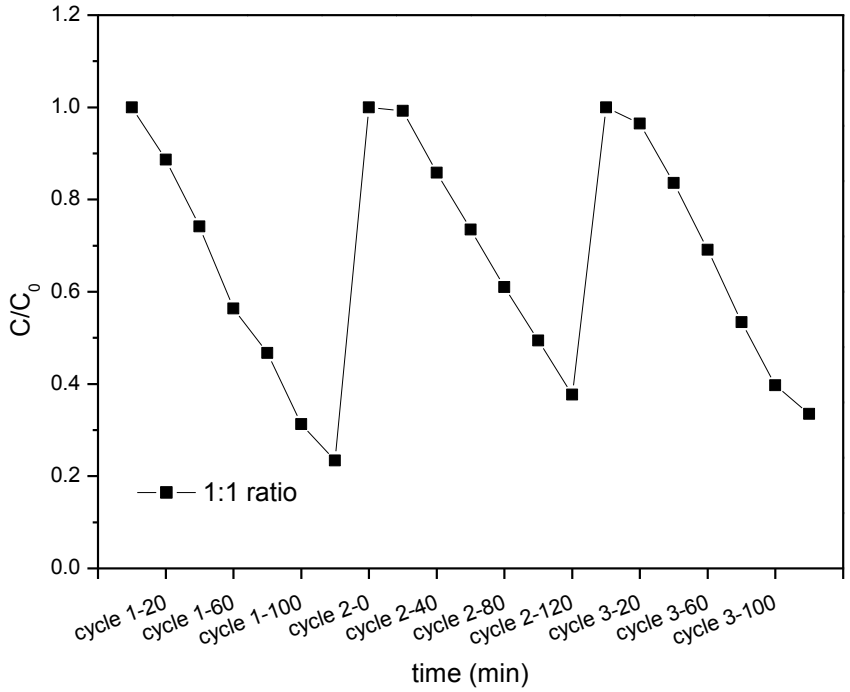

Figure 19. Photocatalytic efficiency of hybrid films with 1:1 ratio in 3 cycles of testing. (Cycle n-m meant m minutes of reactions in cycle n)

Table 8. Mass changes of hybrid films with 1:1 ratio during 3 cycles of testing.

Samples	Mass (g)		
	Before experiment	After experiment	Difference
Cycle 1	1.1642	1.1632	0.0010
Cycle 2	1.1632	1.1632	0
Cycle 3	1.1632	1.1626	0.0006

On the other hand, the performance of film with 1:2 feed ratio decreased as the cycles went on. After three cycles, the mass loss had been accumulated to be more

than 0.0030 g and less than 70% MB could be degraded (Figure 20 and Table 9). This observation once again suggested that excess PVA addition would lead to instability of the prepared films.

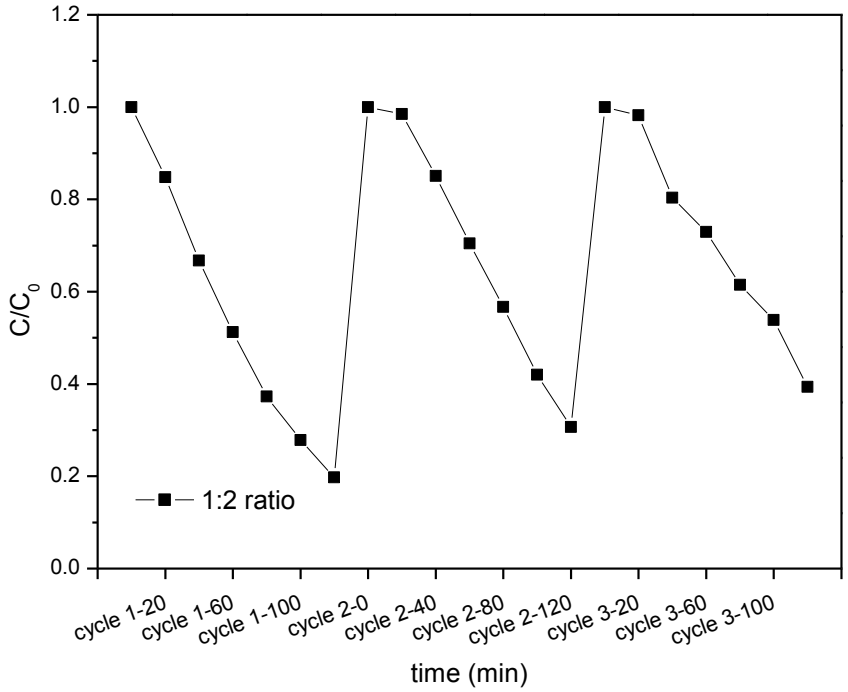

Figure 20. Photocatalytic efficiency of hybrid films with 1:2 ratio in 3 cycles of testing. (Cycle n-m meant m minutes of reactions in cycle n)

Table 9. Mass changes of hybrid films with 1:2 ratio during 3 cycles of testing.

Samples	Mass (g)		
	Before experiment	After experiment	Difference
Cycle 1	1.1585	1.1565	0.0020
Cycle 2	1.1565	1.1563	0.0002
Cycle 3	1.1563	1.1553	0.0010

4.4 Optimization of the solution volume

For the economical application of the drop cast solution, less liquid volume and high solid density of the final solution may be desirable. In this section, we attempted to reduce the solution volume from 30 mL to 25 mL and 20 mL, as listed in Table 10.

Table 10. Preparation parameters of hybrid films made from different solution volumes.

Sample	PVA	P25	Ratio	Solution volume	Film thickness*	Curing temperature
4-1	0.125 g	0.125 g	1:1	30 mL	0.25 mL	150℃
4-2	0.125 g	0.125 g	1:1	25 mL	0.25 mL	150℃
4-3	0.125 g	0.125 g	1:1	20 mL	0.25 mL	150℃

*: Film thickness was controlled by the drop volume of dropcast solution.

Results showed that films made from 30 mL solution volume have higher photocatalytic efficiency (Figure 21). As the solution volume decreased from 30 mL to 20 mL, the degradation of MB went down from 80% to less than 35% within 120 min. Also, considering the mass changes of the hybrid films before and after the photocatalytic reaction, less solution volume led to more mass loss (Table 11). Thus, the optimal solution volume used for the synthesis procedure is found to be 30 mL.

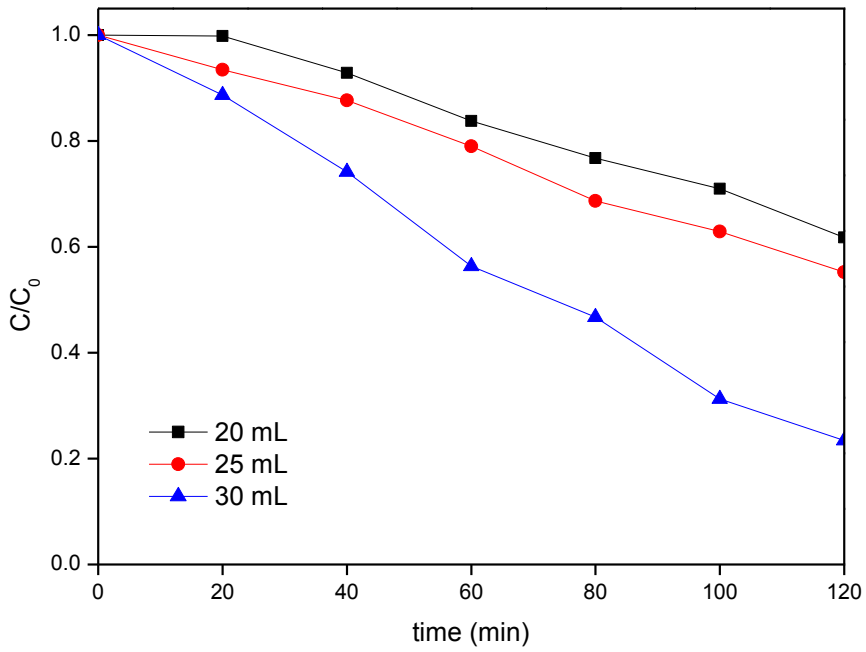

Figure 21. The photocatalytic efficiency of hybrid films made from different solution volumes.

Table 11. Mass changes of the hybrid films before and after the photocatalytic reaction.

Sample	Mass (g)		
	Before experiment	After experiment	Difference
20 mL	1.1196	1.1175	0.0021
25 mL	1.1556	1.1543	0.0013
30 mL	1.1642	1.1632	0.0010

The morphology and transparency of hybrid films made from 20 mL and 25 mL solution volume are also less ideal, as shown in Figure 22 and 23. The hybrid film made from 30 ml solution volume showed obviously better porous microstructure and

transparency. Once contacting with pollutants, the hybrid film could supply more surface area and layers of photocatalyst for the reaction to proceed effectively. Thicker and denser films apparently gave poor optical properties and photocatalytic activity.

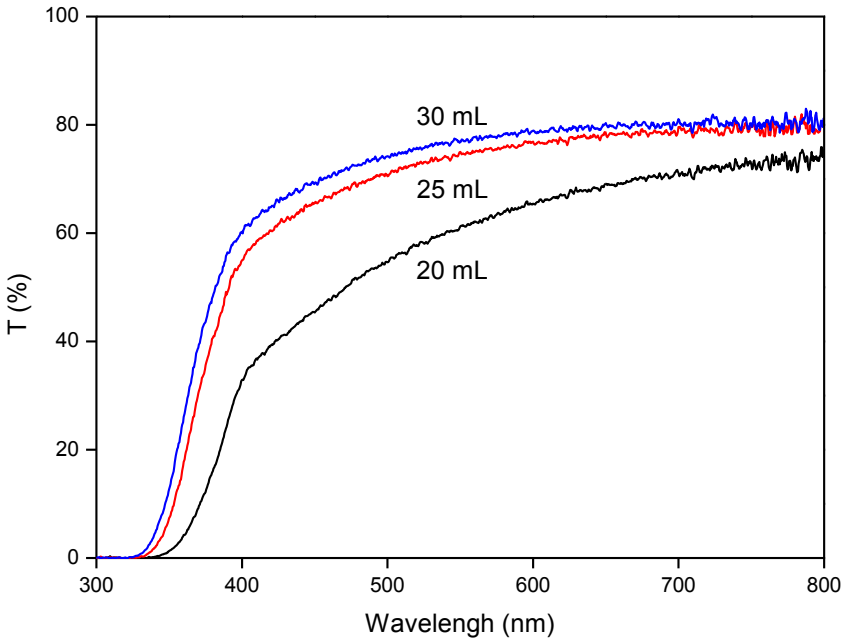

Figure 22. The transparency property of hybrid films made from different solution volumes.

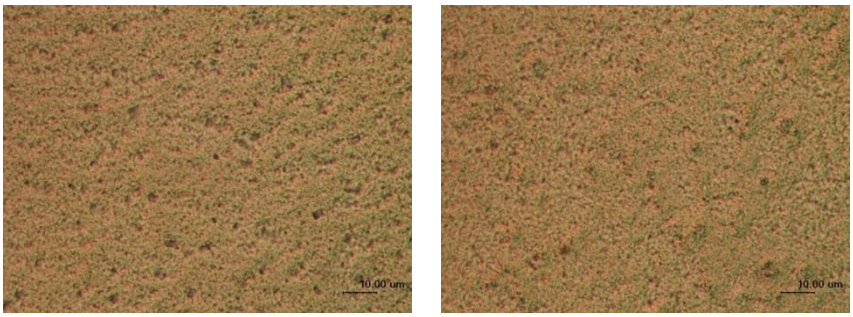

(a) 30 mL (b) 25 mL

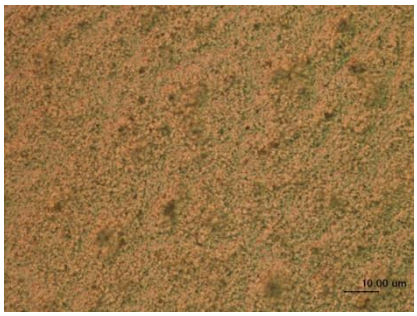

(c) 20 mL

Figure 23. Microscopic images of hybrid films made from different solution volumes: (a) 30 mL, (b) 25 mL and (c) 20 mL.

Chapter 5 FURTHER TEST

On the basis of optimum curing temperature, film thickness, P25/PVA feed ratio and solution volume studied above, we proceeded to examine the optimized hybrid films for microbial, mechanical and other organic dyes tests.

5.1 Microbial test

E.coli K 12 was used as a typical microbacterial to test the inactivation ability of the photocatalyst. Results showed that within 45 min's of solar irradiation, the hybrid films killed *E.coli* K 12 without any residues, while the number of *E.coli* K 12 in control setup still maintained around 1000 CFU/mL (Figure 24, inset).

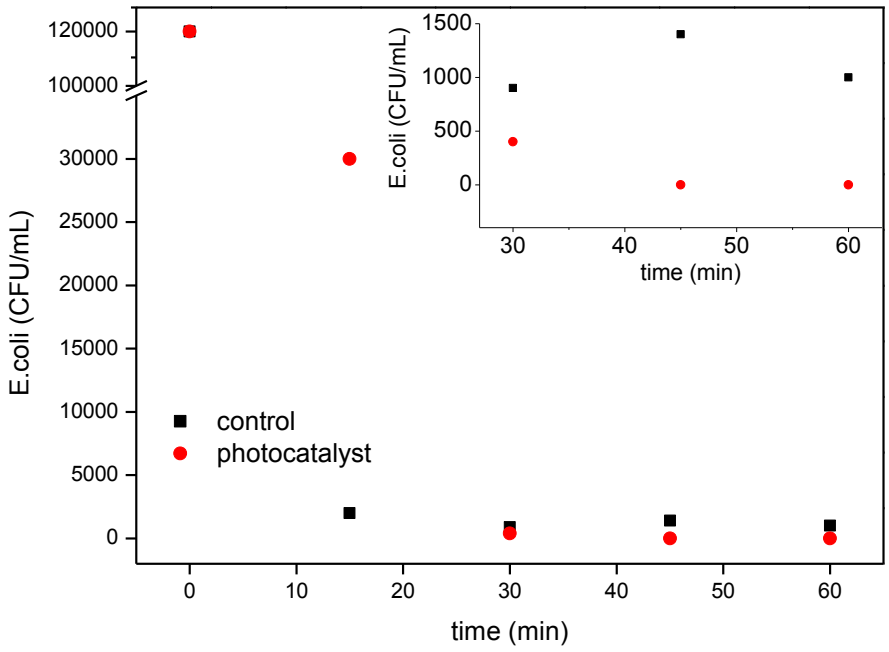

Figure 24. The *E.coli* inactivation ability of the hybrid films.

However, in Tian et al.'s research, 94% of *E.coli* K12 could still be detected in the setup without photocatalyst, much higher than our data in Figure 24[30]. We suspect this is due to the different irradiation conditions used. In this project, simulated solar light was used without any filter. The existence of UV ray and strong irradiation condition may have contributed to the inactivation of *E.coli* K12, even without photocatalyst addition.

5.2 Mechanical test

Besides good inactivation ability, the hybrid films also showed good stability under stirring environment. As listed in Table 12, with the increase of stirring rate from 200 rpm to 300 rpm, the hybrid films remained relatively stable. However, once the stirring rate was increased beyond 400 rpm, the films began to be destroyed gradually with more mass loss after the stirring process.

Furthermore, we also subjected the hybrid films under 300 rpm stirring environment for prolong period of time. As shown in Table 13, the films could still remain relatively stable without apparent damages even after 24 h of stirring. The optimized conditions thus produced hybrid films with very good mechanical properties.

Table 12. Mass changes of the hybrid films at different stirring rate for 1 h.

Samples	Mass (g)		
	Before experiment	After experiment	Difference
200 rpm	1.1368	1.1361	0.0007
300 rpm	1.1489	1.1482	0.0007
400 rpm	1.1555	1.1546	0.0009
500 rpm	1.1634	1.1621	0.0013
600 rpm	0.9983	0.9969	0.0014

Table 13. Mass changes of the hybrid films at 300 rpm for different time length.

Samples	Mass (g)		
	Before experiment	After experiment	Difference
1 h	1.1489	1.1482	0.0007
2 h	1.1186	1.116	0.0010
4 h	1.0915	1.0910	0.0005
6 h	1.0732	1.0722	0.0010
18 h	1.0366	1.0356	0.0010
24 h	1.1204	1.1198	0.0006

5.3 Other organic dyes test

As a further testing of organic dyes, the degradation of RhB was carried out with

the optimized hybrid films. As illustrated in Figure 25, the RhB decay process could be divided into two stages, i.e. a lag-phase (0-30 min) and an accelerated liner degradation phase (30-240 min). The hybrid films showed good photocatalytic efficiency on RhB with the dye degraded to less than 20% within 280 min. This result is comparable to Song et al.'s research [48].

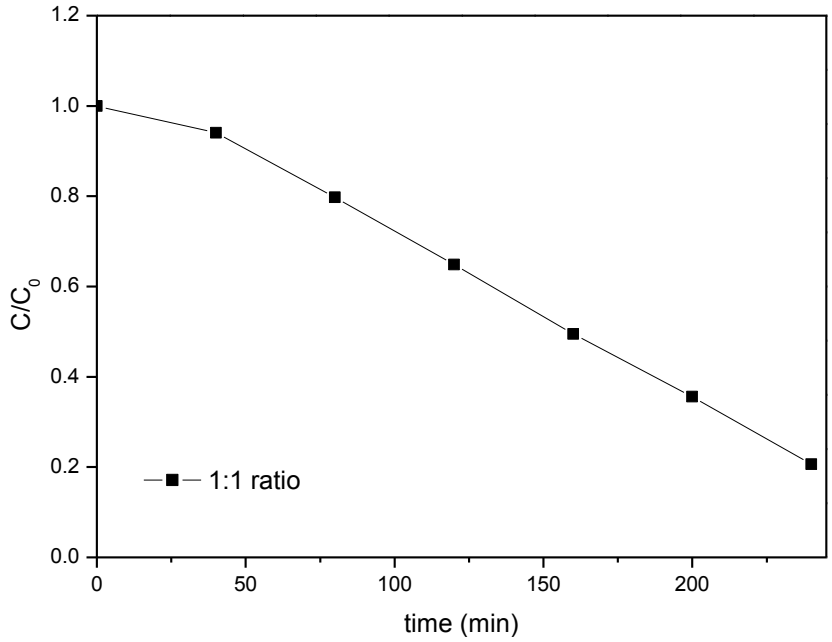

Figure 25. The photocatalytic efficiency of the optimized hybrid films on RhB.

Chapter 6 CONCLUSIONS AND RECOMMENDATIONS

6.1 Conclusions

In our study, some important results were obtained, as listed in the following:

a). The optimal choice of curing temperature, film thickness, the feed ratio of P25/PVA and solution volume during the synthesis process are 150 ℃, 0.25 mL, 1:1 and 30 mL. Under that condition, the hybrid films could perform well and remain stable in photocatalytic reaction.

b). Thermal treatment mainly affects the PVA component, while P25 provided some slight differences to the resultant cast films.

c). The linkage of PVA and P25 could be realized by thermal treatment. However, too high temperature was harmful to the films.

d). The optimized hybrid films could have good inactivation capacity and mechanical property. However, stirring rate should not be over 400 rpm.

6.2 Recommendations

For the application of P25/PVA hybrid films, more work need to be done and further optimization could be made from the following two aspects:

a) Replace P25 with other modified TiO_2;

b) Design a proper system for films' application.

REFERENCES

[1]. Programme W. W. A. (2003) *United Nations World Water Development Report*: *Unesco Pub*.

[2]. Council W. W. *Home WWC/Water at a glance/Water Crisis*.

[3]. Zouboulis A., Lazaridis N., Grohmann A. (2002) *Toxic metals removal from waste waters by upflow filtration with floating filter medium. I*. **The case of zinc. Separation science and technology** 37(2), 403-416.

[4]. Tan L.,Sudak R. G. (1992) *Removing color from a groundwater source*. **Journal (American Water Works Association)**, 79-87.

[5]. Nicolet L.,Rott U. (1999) *Recirculation of powdered activated carbon for the adsorption of dyes in municipal wastewater treatment plants*. **Water science and technology** 40(1), 191-198.

[6]. Johnson A. C.,Sumpter J. P. (2001) *Removal of endocrine-disrupting chemicals in activated sludge treatment works*. **Environmental Science & Technology** 35(24), 4697-4703.

[7]. Sabottke C. Y. (2009) *Membrane separation process* , Google Patents.

[8]. LaPara T. M., Konopka A., Nakatsu C. H., et al. (2000) *Thermophilic aerobic wastewater treatment in continuous-flow bioreactors*. **Journal of Environmental Engineering** 126(8), 739-744.

[9]. Bromley-Challenor K., Knapp J., Zhang Z., et al. (2000) *Decolorization of an azo dye by unacclimated activated sludge under anaerobic conditions*. **Water Research** 34(18), 4410-4418.

[10]. Shen H.,Wang Y.-T. (1994) *Biological reduction of chromium by E. coli*. **Journal of Environmental Engineering** 120(3), 560-572.

[11]. Topalov A., Molnar-Gabor D., Kosanić M., et al. (2000) *Photomineralization of the herbicide mecoprop dissolved in water sensitized by TiO_2*. **Water Research** 34(5), 1473-1478.

[12]. Fabian E., Landsiedel R., Ma-Hock L., et al. (2008) *Tissue distribution and toxicity of intravenously administered titanium dioxide nanoparticles in rats*. **Archives of toxicology** 82(3), 151-157.

[13]. Wong C.,Chu W. (2003) *The hydrogen peroxide-assisted photocatalytic degradation of alachlor in TiO_2 suspensions*. **Environmental Science & Technology** 37(10), 2310-2316.

[14]. Ollis D. F., Pelizzetti E., Serpone N. (1991) *Photocatalyzed destruction of water contaminants*. **Environmental Science & Technology** 25(9), 1522-1529.

[15]. Blount M. C., Kim D. H., Falconer J. L. (2001) *Transparent thin-film TiO_2 photocatalysts with high activity*. **Environmental Science & Technology** 35(14), 2988-2994.

[16]. Bekbölet M., Cecen F., Özkösemen G. (1996) *Photocatalytic oxidation and subsequent adsorption characteristics of humic acids*. **Water science and technology** 34(9), 65-72.

[17]. Sanchez L., Peral J., Domenech X. (1997) *Photocatalyzed destruction of aniline in UV-illuminated aqueous TiO_2 suspensions*. **Electrochimica acta** 42(12), 1877-1882.

[18]. Xu Y.,Langford C. H. (2000) *Variation of Langmuir adsorption constant determined for TiO_2-photocatalyzed degradation of acetophenone under different light intensity*. **Journal of Photochemistry and Photobiology A: Chemistry** 133(1), 67-71.

[19]. Aceituno M., Stalikas C. D., Lunar L., et al. (2002) *H_2O_2/TiO_2 photocatalytic oxidation of metol. Identification of intermediates and reaction pathways*. **Water Research** 36(14), 3582-3592.

[20]. Negishi N., Iyoda T., Hashimoto K., et al. (1995) *Preparation of Transparent TiO_2 Thin Film Photocatalyst and Its Photocatalytic Acitivity*. **Chemistry Letters** (9), 841-842.

[21]. Ahmad J., Deshmukh K., Hägg M. B. (2013) *Influence of TiO_2 on the Chemical, Mechanical, and Gas Separation Properties of Polyvinyl Alcohol-Titanium Dioxide (PVA-TiO_2) Nanocomposite Membranes*. **International Journal of Polymer Analysis and Characterization** 18(4),

287-296.

[22]. Sclafani A., Palmisano L., Schiavello M. (1990) *Influence of the preparation methods of titanium dioxide on the photocatalytic degradation of phenol in aqueous dispersion*. **Journal of physical chemistry** 94(2), 829-832.

[23]. Su W., Zhang J., Feng Z., et al. (2008) *Surface phases of TiO_2 nanoparticles studied by UV Raman spectroscopy and FT-IR spectroscopy*. **The Journal of Physical Chemistry C** 112(20), 7710-7716.

[24]. Jiang D., Zhang S., Zhao H. (2007) *Photocatalytic degradation characteristics of different organic compounds at TiO_2 nanoporous film electrodes with mixed anatase/rutile phases*. **Environmental Science & Technology** 41(1), 303-308.

[25]. Anpo M., Shima T., Kodama S., et al. (1987) *Photocatalytic hydrogenation of propyne with water on small-particle titania: size quantization effects and reaction intermediates*. **Journal of physical chemistry** 91(16), 4305-4310.

[26]. Porter J. F., Li Y.-G., Chan C. K. (1999) *The effect of calcination on the microstructural characteristics and photoreactivity of Degussa P-25 TiO_2*. **Journal of materials science** 34(7), 1523-1531.

[27]. Doong R., Maithreepala R., Chang S. (2000) *Heterogeneous and homogeneous photocatalytic degradation of chlorophenolsin aqueous titanium dioxide and ferrous ion*. **Water science & technology** 42(7-8), 253-260.

[28]. Prevot A. B., Vincenti M., Bianciotto A., et al. (1999) *Photocatalytic and*

photolytic transformation of chloramben in aqueous solutions. **Applied Catalysis B: Environmental** 22(2), 149-158.

[29]. Chu W.,Wong C. (2004) *The photocatalytic degradation of dicamba in TiO_2 suspensions with the help of hydrogen peroxide by different near UV irradiations*. **Water Research** 38(4), 1037-1043.

[30]. Tian B., Dong R., Zhang J., et al. (2014) *Sandwich-structured $AgCl@Ag@TiO_2$ with excellent visible-light photocatalytic activity for organic pollutant degradation and E. coli K12 inactivation*. **Applied Catalysis B: Environmental** 158-159, 76-84.

[31]. Satyro S., Marotta R., Clarizia L., et al. (2014) *Removal of EDDS and copper from waters by TiO_2 photocatalysis under simulated UV–solar conditions*. **Chemical Engineering Journal** 251, 257-268.

[32]. Zsilák Z., Szabó-Bárdos E., Fónagy O., et al. (2014) *Degradation of benzenesulfonate by heterogeneous photocatalysis combined with ozonation*. **Catalysis today** 230, 55-60.

[33]. Du F.,Yu S. (2014) *Preparation and Characterization of Zr–N-Codoped TiO_2 Nano-Photocatalyst and Its Activity Enhanced-Mechanism*. **Journal of Nanoscience and Nanotechnology** 14(9), 6965-6969.

[34]. Badawy M., Souaya E. M., Gad‐Allah T. A., et al. (2014) *Fabrication of Ag/TiO_2 photocatalyst for the treatment of simulated hospital wastewater*

under sunlight. **Environmental Progress & Sustainable Energy** 33(3), 886-894.

[35]. Shavisi Y., Sharifnia S., Zendehzaban M., et al. (2014) *Application of solar light for degradation of ammonia in petrochemical wastewater by a floating TiO_2/LECA photocatalyst*. **Journal of Industrial and Engineering Chemistry** 20(5), 2806-2813.

[36]. Xie H., Zheng Q., Wang S., et al. (2014) *Capture of phosphates in surface water by TiO_2 nanoparticles under UV irradiation*. **Particuology** 14, 98-102.

[37]. Zhao F. (2013) *Study on the synthesis, characterization and photocatalystic properties of Ag and N codoped supported titanium dioxide nanoparticles*, NingXia University.

[38]. Matsushita M., Tran T. H., Nosaka A. Y., et al. (2007) *Photo-oxidation mechanism of l-alanine in TiO_2 photocatalytic systems as studied by proton NMR spectroscopy*. **Catalysis today** 120(2), 240-244.

[39]. Klauson D., Budarnaja O., Castellanos Beltran I., et al. (2014) *Photocatalytic decomposition of humic acids in anoxic aqueous solutions producing hydrogen, oxygen and light hydrocarbons*. **Environmental technology** 35(17), 2237-2243.

[40]. Sun W., Chu H., Dong B., et al. (2014) *The Degradation of Naproxen and Diclofenac by a Nano-TiO_2/diatomite Photocatalytic Reactor*. **International**

Journal of Electrochemical Science 9, 4566-4573.

[41]. Cho M., Chung H., Choi W., et al. (2004) *Linear correlation between inactivation of E. coli and OH radical concentration in TiO_2 photocatalytic disinfection*. **Water Research** 38(4), 1069-1077.

[42]. Matsunaga T., Tomoda R., Nakajima T., et al. (1985) *Photoelectrochemical sterilization of microbial cells by semiconductor powders*. **FEMS Microbiology letters** 29(1-2), 211-214.

[43]. Maness P. C., Smolinski S., M.Blake D., et al. (1999) *Bacterial activity of photocatlyticTiO$_2$ reaction: toward an understanding of its killing mechanism*. **Applied and Environmental Microbiology** 65(9), 4094-4098.

[44]. Sjogren J. C.,Sierka R. A. (1994) *Inactivation of phage MS_2 by iron-aided titanium dioxide photocatalysis*. **Applied and Environmental Microbiology** 60(1), 344-347.

[45]. Benabbou A., Derriche Z., Felix C., et al. (2007) *Photocatalytic inactivation of Escherischia coli: Effect of concentration of TiO_2 and microorganism, nature, and intensity of UV irradiation*. **Applied Catalysis B: Environmental** 76(3), 257-263.

[46]. Cho M., Chung H., Choi W., et al. (2004) *Linear correlation between inactivation of E. coli and OH radical concentration in TiO_2 photocatalytic disinfection*. **Water Research** 38(4), 1069-77.

[47]. Rincon A. G.,Pulgarin C. (2004) *Effect of pH, inorganic ions, organic matter and H_2O_2 on E. coli K12 photocatalytic inactivation by TiO_2: implications in solar water disinfection*. **Applied Catalysis B: Environmenta**l 51(4), 283-302.

[48]. Song Y., Zhang J., Yang H., et al. (2014) *Preparation and visible light-induced photo-catalytic activity of H-PVA/TiO_2 composite loaded on glass via sol–gel method*. **Applied Surface Science** 292, 978-985.

[49]. Li D., Haneda H., Hishita S., et al. (2005) *Visible-light-driven NF-codoped TiO_2 photocatalysts. 2. Optical characterization, photocatalysis, and potential application to air purification*. **Chemistry of Materials** 17(10), 2596-2602.

[50]. Wang X., Jimmy C. Y., Liu P., et al. (2006) *Probing of photocatalytic surface sites on SO_4^{2-}/TiO_2 solid acids by in situ FT-IR spectroscopy and pyridine adsorption*. **Journal of Photochemistry and Photobiology A: Chemistry** 179(3), 339-347.

[51]. Gelover S., Mondragón P., Jiménez A. (2004) *Titanium dioxide sol–gel deposited over glass and its application as a photocatalyst for water decontamination*. **Journal of Photochemistry and Photobiology A: Chemistry** 165(1), 241-246.

[52]. KIEDA N.,TOKUHISA T. (2006) *Immobilization of TiO_2 photocatalyst particles on stainless steel substrates by electrolytically deposited Pd and Cu*.

Nippon seramikkusu kyokai gakujutsu ronbunshi 114(1), 42-45.

[53]. Zeng J., Liu S., Cai J., et al. (2010) *TiO_2 immobilized in cellulose matrix for photocatalytic degradation of phenol under weak UV light irradiation*. **The Journal of Physical Chemistry C** 114(17), 7806-7811.

[54]. Lei P., Wang F., Gao X., et al. (2012) *Immobilization of TiO_2 nanoparticles in polymeric substrates by chemical bonding for multi-cycle photodegradation of organic pollutants*. **Journal of hazardous materials** 227, 185-194.

[55]. Ng J., Wang X., Sun D. D. (2011) *One-pot hydrothermal synthesis of a hierarchical nanofungus-like anatase TiO_2 thin film for photocatalytic oxidation of bisphenol A*. **Applied Catalysis B: Environmental** 110, 260-272.

[56]. Pang Y. L., Lim S., Ong H. C., et al. (2014) *A critical review on the recent progress of synthesizing techniques and fabrication of TiO_2-based nanotubes photocatalysts*. **Applied Catalysis A: General** 481, 127-142.

[57]. Zhang X., Pan J. H., Du A. J., et al. (2009) *Combination of one-dimensional TiO_2 nanowire photocatalytic oxidation with microfiltration for water treatment*. **Water Research** 43(5), 1179-1186.

[58]. Sun D. D., Lee P. F., Leckie J. O. (2007) *Microspheric TiO_2 photocatalyst*, Google Patents.

[59]. Jaroenworaluck A., Sunsaneeyametha W., Kosachan N., et al. (2006) *Characteristics of silica‐coated TiO_2 and its UV absorption for sunscreen*

cosmetic applications. **Surface and Interface Analysis** 38(4), 473-477.

[60]. Xu Q. C., Wellia D. V., Sk M. A., et al. (2010) *Transparent visible light activated C–N–F-codoped TiO_2 films for self-cleaning applications*. **Journal of Photochemistry and Photobiology A: Chemistry** 210(2), 181-187.

[61]. Subianto H., Nuryadin B. W., Khairurrijal, et al. (2013) *Distributed inner states TiO_2-coated plastic fibers as photocatalysts for decomposing organic pollutants in water*. **Journal of Material Cycles and Waste Management** 15(2), 210-217.

[62]. Liu X., Chen Q., Lv L., et al. (2015) *Preparation of transparent PVA/TiO_2 nanocomposite films with enhanced visible-light photocatalytic activity*. **Catalysis Communications** 58, 30-33.

[63]. Antonello A., Soliveri G., Meroni D., et al. (2014) *Photocatalytic remediation of indoor pollution by transparent TiO_2 films*. **Catalysis today** 230, 35-40.

[64]. Ahmadpoor P., Nateri A. S., Motaghitalab V. (2013) *The optical properties of PVA/TiO_2 composite nanofibers*. **Journal of Applied Polymer Scienc**e 130(1), 78-85.

[65]. Wang Y., Zhong M., Chen F., et al. (2009) *Visible light photocatalytic activity of TiO_2/D-PVA for MO degradation*. **Applied Catalysis B: Environmental** 90(1-2), 249-254.

[66]. Prosanov I. Y., Matvienko A. A. (2010) *Study of PVA thermal destruction by*

means of IR and Raman spectroscopy. **Physics of the Solid State** 52(10), 2203-2206.

[67]. Gohil J., Bhattacharya A., Ray P. (2006) *Studies on the crosslinking of poly (vinyl alcohol)*. **Journal of polymer research** 13(2), 161-169.

[68]. Tada H.,Tanaka M. (1997) *Dependence of TiO_2 photocatalytic activity upon its film thickness*. **Langmuir** 13(2), 360-364.

[69]. Yu J., Zhao X., Zhao Q. (2000) *Effect of film thickness on the grain size and photocatalytic activity of the sol-gel derived nanometer TiO_2 thin films*. **Journal of materials science letters** 19(12), 1015-1017.

[70]. Chen Y.,Dionysiou D. D. (2006) *Correlation of structural properties and film thickness to photocatalytic activity of thick TiO_2 films coated on stainless steel*. **Applied Catalysis B: Environmental** 69(1-2), 24-33.

[71]. Maurya A.,Chauhan P. (2012) *Synthesis and characterization of sol–gel derived PVA-titanium dioxide (TiO_2) nanocomposite*. **Polymer bulletin** 68(4), 961-972.

[72]. Kadem B. Y. (2011) *Study of some mechanical properties of PVA/TiO_2 composite by ultrasonic technique*. **International Journal of Science and Technology** 1(5), 183-188.